

ScholarWorks@GSU

Paleoenvironmental and Paleoclimatic Changes in Tropical East Africa Since the LGM: New Record from the Cherangani Hills Kenya

Authors	Opiyo, Benjamin Atieno
Citation	Opiyo, Benjamin Atieno. Paleoenvironmental and Paleoclimatic Changes in Tropical East Africa Since the LGM: New Record from the Cherangani Hills Kenya. Dec. 2018, Georgia State University. https://doi.org/10.57709/13426136 .
DOI	https://doi.org/10.57709/13426136
Download date	2026-06-06 20:32:54
Link to Item	https://hdl.handle.net/20.500.14694/6319

PALEOENVIRONMENTAL AND PALEOCLIMATIC CHANGES IN TROPICAL EAST
AFRICA SINCE THE LGM: NEW RECORD FROM THE CHERANGANI HILLS KENYA.

by

BENJAMIN OPIYO

Under the Direction of Lawrence M. Kiage, PhD

ABSTRACT

A 3.5 m radiocarbon-dated sediment core was recovered from the Kapkanyar mire, Cherangani Hills, Kenya, to reconstruct the paleoclimatic and paleoenvironmental variations in Tropical East Africa since the last glacial maxima. Through a multi-proxy approach of pollen, elemental geochemistry, and LOI analysis, different deductions were made based on the relationship of the patterns exhibited by each proxy. Associations of varying pollen type groupings: the arboreal, herbaceous and shrubs were used to infer the prevailing paleoclimates considering the vegetation-climate relationship that has been observed and exploited in pioneering palynological studies. Findings from this study reveal notable climate dynamics of sub-orbital scale global climate signals including the East African monsoon signals, the African Humid period (16Ka-6Ka) and Pleistocene aridity events such as the Younger Dryas (14Ka-12Ka). Although anthropogenic activities are observed to be a principal driver in environmental change, it is evident that they do not entirely oust natural background climatic changes.

INDEX WORDS: Cherangani Hills, Tropical Africa, Pollen, Younger-Dryas, Last-Glacial-Maximum, African-Humid-Period.

PALEOENVIRONMENTAL AND PALEOCLIMATIC CHANGES IN TROPICAL EAST
AFRICA SINCE THE LGM: NEW RECORD FROM THE CHERANGANI HILLS KENYA.

by

BENJAMIN OPIYO

A Thesis Submitted in Partial Fulfillment of the Requirements for the Degree of

Master of Science

in the College of Arts and Sciences

Georgia State University

2018

Copyright by
Benjamin Atieno Opiyo
2018

PALEOENVIRONMENTAL AND PALEOCLIMATIC CHANGES IN TROPICAL EAST
AFRICA SINCE THE LGM: NEW RECORD FROM THE CHERANGANI HILLS KENYA

by

BENJAMIN OPIYO

Committee Chair: Lawrence Kiage

Committee: Daniel Deocampo

Brian Meyer

Electronic Version Approved:

Office of Graduate Studies

College of Arts and Sciences

Georgia State University

December, 2018

DEDICATION

I would like to dedicate this work to my dad and mom, Mr. Isaiah Opiyo and Mrs. Catherine Opiyo, for their never-ending prayers and support and my twin sisters, Brenda Opiyo and Bridgit Opiyo, who have always looked up to me as their role model. I love you guys.

ACKNOWLEDGEMENTS

I would like to appreciate the funding from the National Science Foundation (NSF) for the project and the support and guidance of my advisor Dr. Lawrence Kiage who has always believed that I can do better as long as I put my nose to the grindstone and work at it. Thanks to my thesis committee Dr. Deocampo and Dr. Meyer for the help accorded through the whole process and preparation of this document. Thank you Dr. Gebregiorgis for the immense support and a keen eye for detail throughout the preparation and combing of this document. A big thank you to the Geosciences department for the graduate research and teaching assistant positions they offered me; which enabled me to finance my masters' education to a successful completion. Great appreciation too to my colleagues and course mates especially Francis Muchemi who has been a friend, elder brother and mentor whom we started the journey for our studies abroad in The United States together and has always supported me in all my academic and life engagements. A big thank you to Vicky Chelang'at whom we worked in the lab together through the tedious palynological work. Not to forget Mr. Muchiri, great thanks for driving us through the challenging Cherangani Hills terrain during the coring field excursions.

TABLE OF CONTENTS

ACKNOWLEDGEMENTS	V
LIST OF TABLES	VIII
LIST OF FIGURES	IX
LIST OF ABBREVIATIONS	XI
1 INTRODUCTION	1
1.1 Study Area	3
1.2 Research Question.....	6
2 METHODS.....	7
2.1 Coring.....	7
2.2 Loss-On-Ignition Analysis (LOI)	8
2.3 X-Ray Fluorescence.....	9
2.4 Dating of Core Sediments	9
2.5 Palynological analysis	9
3 RESULTS.....	11
3.1 Core Chronology	11
3.2 LOI and Lithostratigraphy	12
3.3 Pollen	15
3.4 Charcoal	20
4 DISCUSSION.....	25

5 CONCLUSIONS..... 35

REFERENCES..... 36

LIST OF TABLES

Table 1: Table of the AMS radiocarbon chronology for the Kapkanyar Core used to develop the age model and the different materials sampled at each level. The calibrated dates were generated using the Calib 6.0 program (Reimer, 2013 ; Stuiver et al., 2005) The ages in red within the table were not used for the initial generation of the age model.	11
Table 2: An exhaustive list of all the pollen types and spores identified in the Kapkanyar Swamp Core.	17

LIST OF FIGURES

- Figure 1: Location of the Cherangani Hills watershed site location in Kenya relative to other paleolakes where previous works have been conducted along the Gregorian Rift Valley from subsets of East African region and African continent maps (red outline on the Kenyan map marks the site)..... 5
- Figure 2:Field images showing the Modified Livingstone Corer used to recover sediment. 7
- Figure 3: Systematic illustration showing the steps involved in Loss on Ignition analysis (LOI). 8
- Figure 4:Figure Showing the fume hood used in acid treatment and acetolysis in the Lab. 10
- Figure 5:Age Control Model generated using three of the four calibrated radiocarbon ages marked by red dots with a purple ring, obtained from the AMS. Yellow dots are affirmative additional dates that line up with the age model. The markers show the depth and calibrated ages for the dated organic materials.)..... 12
- Figure 6: Sediment LOI and Lithostratigraphy data of the Kapkanyar Core Showing percentage (%)water, organics, carbonates patterns with their relative C14 ages and depth along the core..... 15
- Figure 7:Pollen diagram showing percentage calculations of relative abundance of pollen with five dendrograms showing distinct pollen assemblage zonation based on the CONNISS classification. The colored dots represent presence of grains below 3% threshold for representation as bars..... 18
- Figure 8: Illustration of wetness dynamics as depicted from the proportions of the Cyperaceae to Poaceae pollen throughout the record.(numbers on bars indicate the pollen counts)..... 19
- Figure 9:A figure showing charcoal representation and abundance down the Kapkanyar core used to develop possible fire regime of the Kapkanyar site. 21

Figure 10:Kapkanyar Core XRF spectrum showing down the core concentrations of selected elements useful for paleoclimatic interpretations with changing lithology. 22

Figure 11: A matrix of correlation showing pair of elements with the highest R2 value (Zr vs. Ti) 24

LIST OF ABBREVIATIONS

AMS Accelerator Mass Spectrometry

ENSO El Niño-Southern Oscillation

LGM Last Glacial Maxima

XRF X-ray Fluorescence

LOI Loss on ignition

ITCZ Inter-Tropical Convergence Zone

BP Before Present

Ka Thousand Years

Cm³ Cubic Centimeters

µm micrometers

1 INTRODUCTION

East Africa is made of an assortment of environments ranging from arid and semiarid to humid mountainous ranges and tropical forests to Savannah grasslands. Unique vegetation assemblages also referred to as biomes, accompany each of these environments (Izumi and Lézine, 2016). Cumulative effects of both human influence and natural climatic variations have been a primary control and sculptor of the dominant type of vegetation in the landscapes. These different vegetation communities have experienced increased pressure from the exponentially growing population in the region. Even though human activities have taken precedence in shaping the current vegetation cover in East Africa, it does not oust the effect of the regional climatic regime (Marchant et al., 2018).

Vegetation change mirrors change in climate and environmental conditions whether they owe their source to anthropogenic activities or natural background climatic variations (Bush and Colinvaux, 1990; Courtney Mustaphi et al., 2017; Ivory and Russell, 2016; Izumi and Lézine, 2016; Kiage and Liu, 2009; Novenko et al., 2018; Sánchez Goñi et al., 2017; Schüller et al., 2012; Tian et al., 2017). Climatic variations result in alterations in the amount of water inflows, outflows and storage within a hydrological cycle: which are the essential components of a hydrological budget and this results in ever-changing hydrological budgets. The hydrological cycle responds differently to these climatic and environmental variations depending on an area's level of fragility, which is referred to as the hydrological sensitivity. With the different hydrological budgets that have been experienced in the East African region through time (Tierney et al., 2011), it is also expected that the vegetation will mimic their dynamics.

The orography of the East African landscapes, on the other hand, has played a principal role in enhancing the complexity of the hydrological sensitivity of different areas that may be in

very close geographical proximity and consequently the vegetation cover (Gasse, 2000; Oettli and Camberlin, 2005). This could lead to erroneous climatic interpretations and correlations over wide regions. Apart from the three controls mentioned above, a confluence of other processes including solar activity and changes in insolation, atmospheric composition and circulation, teleconnections including El Niño-Southern Oscillation (ENSO) events and ocean currents also account for the climate variations experienced in this region (Marchant et al., 2018). This, therefore, convolutes the efforts of trying to disentangle the critical controls of the East African climate, hence the need for a good choice of climate proxy (Kiage and Liu, 2009).

Vegetation is an ideal yardstick for the environmental changes since it is a manifestation of the prevailing climatic and ecological conditions (Quick et al., 2011). Consequently, pollen archived in lithological sediment records through sedimentation and deposition processes can actively aid in shedding light on past environments by providing vegetation histories through time (Izumi and Lézine, 2016; Tian et al., 2017). The vegetation-climate relationship has proven to be reliable, given that different vegetation assemblages and their distribution are representative of an ideal set of conditions of temperature, moisture, solar radiation, soils, carbon dioxide levels, winds, biotic interactions and forms of disturbances experienced such as fires and other anthropogenic activities.

We present a new high-resolution record of pollen and elemental geochemistry data that elucidate the environmental changes from the terminus stage of the latest glacial maxima to the present. Although a number of studies (Battistel et al., 2017; Berke et al., 2014; Courtney Mustaphi et al., 2017; Foerster et al., 2012; Foerster et al., 2015; Rucina et al., 2009), have been performed in different locations throughout the East African region, in some situations the question still remains as to whether the interpreted results are regional mostly as a result of prevailing climates

or site-specific either due to microclimates as a result of complex orography (Oettli and Camberlin, 2005) or anthropogenic activities (Wright, 2017). An earlier record (Coetzee, 1967) obtained from Kaisungor Swamp, near the study area has the challenge of hiatuses but it provides a good background to build on for this research.

1.1 Study Area

The Cherangani Hills stand as lofty highly folded residual erosional ranges on the Southeastern part of Pokot County in Western Kenya (Fig 1). The area has a lot of rugged, steep slopes averaging a height of around 3300 meters (m) above sea level. Its geology is typically a metamorphic terrain occupied by Precambrian rocks of the basement system mostly granitoid gneisses and schists, and intercalated with prominent quartzite ridges with occasional marble veins (Strategic Ecosystem Management Plan 2015-2040). These forests are the primary catchment areas for the rivers Turkwel, Nzoia and Kerio playing a vital role in maintaining their perennial flow.

The climate of the area is sub-humid, pigeonholed by relatively high temperatures (25-30°C) and an annual mean rainfall of about 1300 millimeters (mm) throughout the year with highest values when the Intertropical Convergence Zone (ITCZ) crosses the equator (Liu et al., 2017). It has some tropical rainforest characteristics with torrential downpours late in the evenings and tall trees at least 30m in height.

The location where the cores were collected, is located at approximately 1°07'07.602" N latitude and 35°17'39.03" E longitude, in a high altitude mire in the Kapcherop Forest Reserve block. This forest block is one of the more consolidated forest blocks alongside the Kapolet and Kiptaberr forest blocks as compared to the others that are fragmented and interspersed by cropland, grasslands, and bushlands, which are indicators of disturbance. The unperturbed sediments of the

Kapkanyar mire made it an excellent site for pollen preservation. The suitability of this site for the study is its hydrological sensitivity to climate variability and the fact that there are no infrastructural developments in the area. Current vegetation cover types and composition on these hills vary with its aspect. *Juniperus-Nuxia-Podocarpus falcatus* forests dominate the South-facing slopes on the Eastern side while the Western facing slopes show the same forest composition interspersed with *Podocarpus falcatus* forests which show higher levels of human disturbance. *Aningeria-Strombosia-Drypetes* forests ecotoning into mixed *Podocarpus latifolius* dominate the West-facing slopes in lower elevations. Steep valleys exhibit material relics of *Juniperus-Maytenus undata-Rapanea-Hagenia* forests while stream valleys have stream valley tree ferns mostly *Cyathea manniana* (Strategic Ecosystem Management Plan 2015-2040).

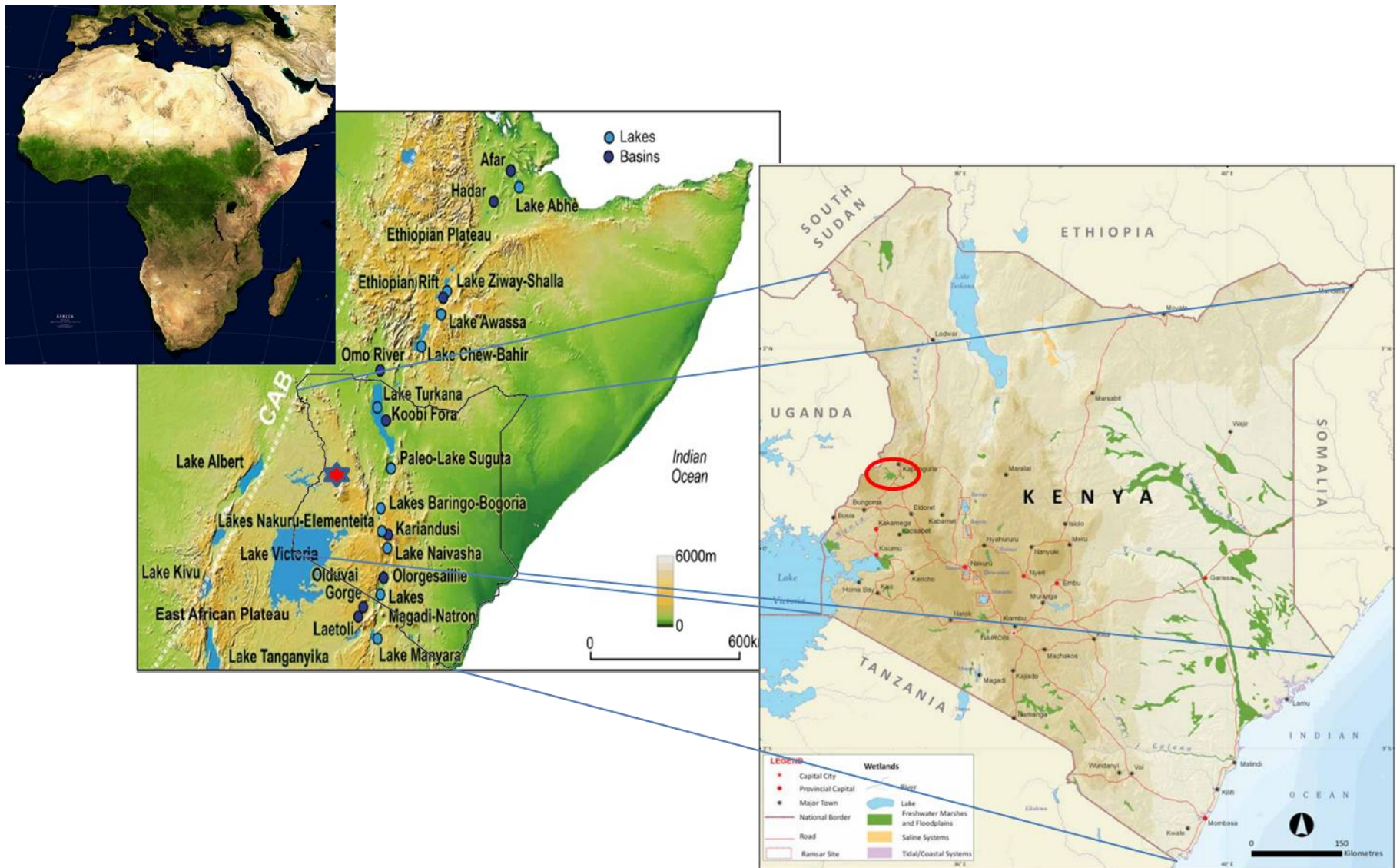


Figure 1: Location of the Cherangani Hills watershed site location in Kenya relative to other paleolakes where previous works have been conducted along the Gregorian Rift Valley from subsets of East African region and African continent maps (red outline on the Kenyan map marks the site).

1.2 Research Question

This study is structured around the following questions: What is the interplay of humans and climate on environmental change in East Africa? Is there an anthropogenic imprint on the environment ousting natural climatic change trend in the region during the last 3000-4500yrs as documented in previous literature? At what point do humans start impacting the environment in East Africa? Is there any confluence of proxies supporting the idea?

2 METHODS

2.1 Coring

Cores from different carefully selected sites in the Cherangani Hills (Kapkanyar and Saiwa Swamps) were obtained using a modified Livingstone Piston corer used in Kiage and Liu, (2009) where three overlapping cores with an overlap of approximately 10 cm were warily extruded. All the core sections were cautiously labeled, described, and preserved in transparent-PVC tubes that were carefully sealed airtight on both ends on site and shipped to Georgia State University Department of Geosciences palynology and geochemistry laboratories for processing and analysis. This coring method was applied since the upper 5 to 10 cm of the mire sediment was invariably very soft, water-saturated and flocculent which would have made it difficult to raise an undisturbed core using other methods. In the laboratories, each core was longitudinally split into two halves using a table saw, photographed, and macroscopically described. The cores were then subjected to high-resolution palynological and sedimentological analysis.



Figure 2: Field images showing the Modified Livingstone Corer used to recover sediment.

2.2 Loss-On-Ignition Analysis (LOI)

1 cm³ samples were taken consecutively throughout the cores at 1 cm intervals and subjected to LOI analysis following the techniques described by Beaudoin (2003) and Santisteban et al. (2004). The samples were heated at 105°C overnight to establish the percentage water and then combusted for 1 hour at 550°C and then at 1000°C to establish the organics content and carbonate contents respectively, by sample weight loss.

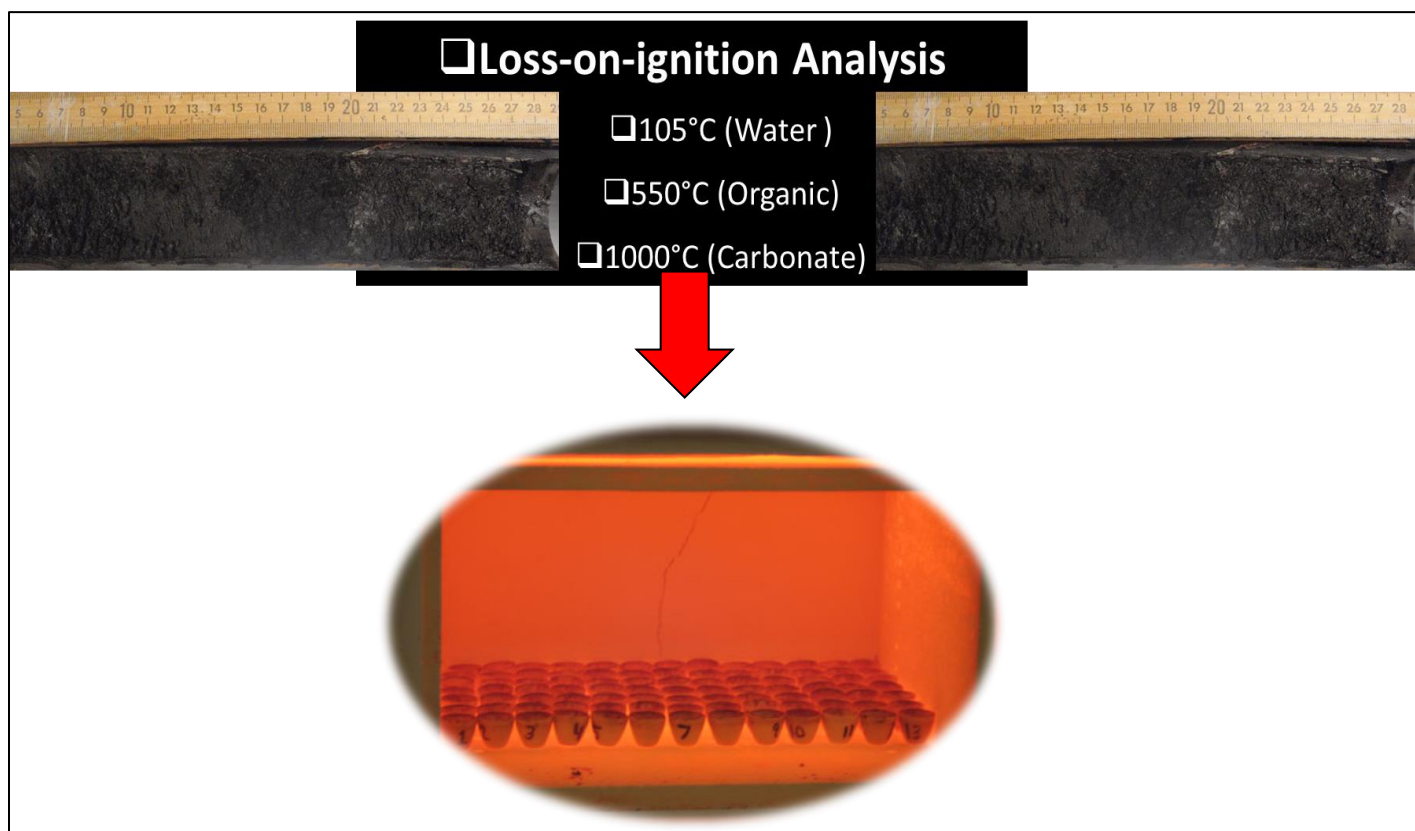


Figure 3: Systematic illustration showing the steps involved in Loss on Ignition analysis (LOI).

2.3 X-Ray Fluorescence

Elemental data for the cores were obtained using a handheld Innov-X Alpha-400 energy dispersive X-ray Fluorescence Spectrometer (XRF). The XRF instrument was set in Soil Analysis mode and run at 60-second cycles twice at every centimeter along the core. The data obtained were then graphed using Tillia plots version 1.7.16 software and Microsoft Excel spreadsheet software (2017). The resulting data were then analyzed and interpreted using chemofacies graphs as shown in Reotita et al., (2014). This was done focusing on the sections of enrichments and depletions of certain index elements, whose ratios are vital for interpretation.

2.4 Dating of Core Sediments

To construct a time-scaled stratigraphic sequence, different sections rich in organic debris along the core were sampled for radiocarbon dating. This was to assist in generating a robust age model for the study. Organic samples were carefully selected throughout the core and sent for Accelerator Mass Spectrometry (AMS) ^{14}C dating at the Direct AMS, Inc. Laboratory in Seattle. The ages established from the dating were then further subjected to an inquiry to inspect for the occurrence of stratigraphic inversion and discontinuity. Using the Bacon based approach, an age model was established employing Matlab 2017 software.

2.5 Palynological analysis

Sediment samples for pollen and microscopic charcoal analysis were taken at intervals ranging from 1-10 cm throughout the core, and a total of 24 samples from the core were prepared for analysis. These samples were sieved and chemically treated to concentrate the materials mentioned above following the standard procedure of Faegri and Iversen (1989). This was accomplished through acid treatment and acid acetolysis, which has proven to be excellent for recovering pollen by dissolving tissue and removing debris. Before pollen processing commenced,

the samples were spiked with *Lycopodium clavatum* spores to aid in the counting and show pollen concentration (Kiage and Liu, 2009). Pollen slides were then prepared out of the processed samples, and then pollen count performed to check for the relative abundance of pollen taxa following the guide in Coetzee (1967) and Faegri and Iversen (1989). Counting of microscopic charcoal and pollen in each slide ceased when a minimum of 300 pollen grains or 1000 *Lycopodium* spores (whichever came first) had been reached (Aleman et al., 2013a; Burney, 1987). Microscopic charcoal that were angular and greater than $4\mu\text{m}$ were considered during counting and great care was taken not to confuse them with biotite mica particles (Rucina et al., 2009).



Figure 4: Figure Showing the fume hood used in acid treatment and acetolysis in the Lab.

3 RESULTS.

3.1 Core Chronology

Table 1 is a summary of the AMS radiocarbon dates of the Kapkanyar Core, the different types of material sampled for dating and their relative depths that appear to have no signs of strata inversion or discontinuity. This was very helpful in developing a Bacon-based age control model for the core (Fig 7). This age control model is ideal since it takes into account the sedimentation rates. It is used to give a control as to the windows in time for the different events such as the occurrence and distribution of microscopic charcoal to come up with a probable fire regime. The radiocarbon samples in the current study were calibrated using CALIB 6.0 software (M. Stuiver and PJ Reimer, 1993) against the IntCal13 database (Reimer et al. 2013) for terrestrial samples. The ^{14}C data were initially corrected for fractionation of carbon isotopes ($\delta^{13}\text{C}$) by normalizing to -25‰ PeeDee Belemnite (PDB). Calibration databases have been constructed using radiocarbon data and absolute dates from dendrochronology and other independently dated samples. Ages generated were used as a primary axis in most of the graphs to ensure proper age constraint for lithology in the record.

Table 1: Table of the AMS radiocarbon chronology for the Kapkanyar Core used to develop the age model and the different materials sampled at each level. The calibrated dates were generated using the Calib 6.0 program (Reimer, 2013 ; Stuiver et al., 2005) The ages in red within the table were not used for the initial generation of the age model.

Depth (cm)	Material Dated	Lab Code	C^{14} Age (BP)	Calibrated Age (Cal Year BP)	2 Sigma Range (Cal Year BP)	$\delta^{13}\text{C}$ (‰)
90	Leaf fragment	D-AMS				
110	Leaf fragment	D-AMS 030332				
178	Leaf fragment	D-AMS 030333	4565±35	3258	5102 - 5313	0.25
228	Leaf fragment	D-AMS 020888	5287±37	4136	4235 - 4020	0.93
254	Leaf fragment	D-AMS 030334	14320±62	15549	17246 - 17751	0.13
300	Leaf fragment	D-AMS 020888	17543±71	19248	19512 - 18984	1
345	Leaf fragment	D-AMS	19597±166	21622	22067 - 21177	1

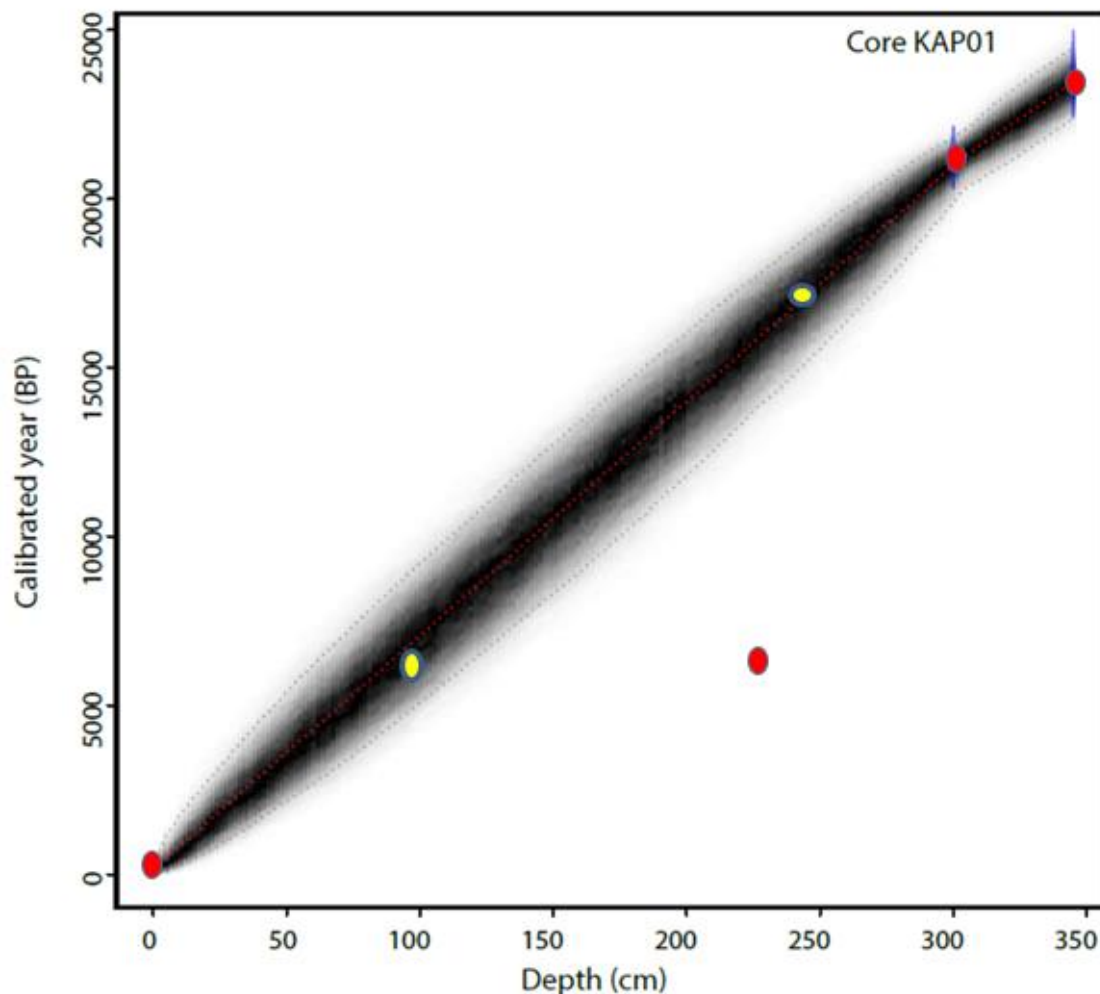


Figure 5: Age Control Model generated using three of the four calibrated radiocarbon ages marked by red dots with a purple ring, obtained from the AMS. Yellow dots are affirmative additional dates that line up with the age model. The markers show the depth and calibrated ages for the dated organic materials.)

3.2 LOI and Lithostratigraphy

The lithostratigraphy of the core is shown in (Fig 6) composed of six principal lithologic units. Similar units such as the different variations of gyttja were grouped as one lithologic unit in the diagram. The bottom section 350- 272 cm is majorly stiff tar-black mud which transitions into brownish gray clay with fossilized wood pieces along the section from 272-232cm which further

transitions with a sharp change in sediment type from 232-222cm to light brownish-yellow sandy stiff clay. This is followed by greyish brown clay with high mica inclusions at around 222-214cm that transitions into greyish black mud with low mica inclusions at 214-198cm. Between 198-100 cm, the core has dark lake mud sediments with no visible organics(198-139cm) that transitions into reduced greyish black lake mud(139-100cm) which is followed by blackish-light brown lake mud from 100-56cm, which further transitions to stiff dark clayey lake mud from around 56-40cm. The top portion between 40 and 0 cm is composed of highly organic dark clayey soil with visible fibrous rootlets.

The LOI data (Fig 6) has been partitioned into five distinct zones (Zone I-V) using the Constrained Incremental Sum of Squares (CONISS), a multivariate package in Tilia, for elaborate description. These zones were also generated considering pollen zonation since it was the major proxy under investigation. Generally, explicit environmental dynamics are seen from the LOI spectrum zoned as having five possible significant paleoenvironmental and paleoclimatic changes throughout the period:

- Zone I (23.5Ka-18Ka), a notable pattern is observed from around 23Ka BP to around 20Ka BP during the LGM; where the levels of organics and water closely correspond to each other while that of the carbonates parallels the two. All are observed to rise but at different stages: water reaches a 40% peak, organics around 10 % and carbonates <5%.
- Zone II (18Ka-12Ka) between approximate ages 19Ka and 16Ka BP there is a relative increase in the levels of carbonates in the core. From around 16Ka to 12Ka there are relatively high levels of organics and water content and very low levels of carbonates.
- Zone III (12Ka-9Ka) spanning around 3K years and partly into the early Holocene. Slightly before 12Ka there is a significant drop in the levels of both water and organics and levels

of carbonates slightly rise. In this early Holocene period at around 9Ka BP there is a sharp substantial drop in the levels of both water and organics and a spike in the level of carbonates.

- Zone IV (9ka-2Ka) is characterized by a plateau phase with intermediate substantial drops in both water and organics and spikes in carbonates at around 6Ka and 3ka.
- Zone V (2Ka-0Ka), which corresponds with the mid-late Holocene period around 2Ka to present, is represented by high levels (%) of water and organics coupled with low levels (%) of carbonates in the sediment.

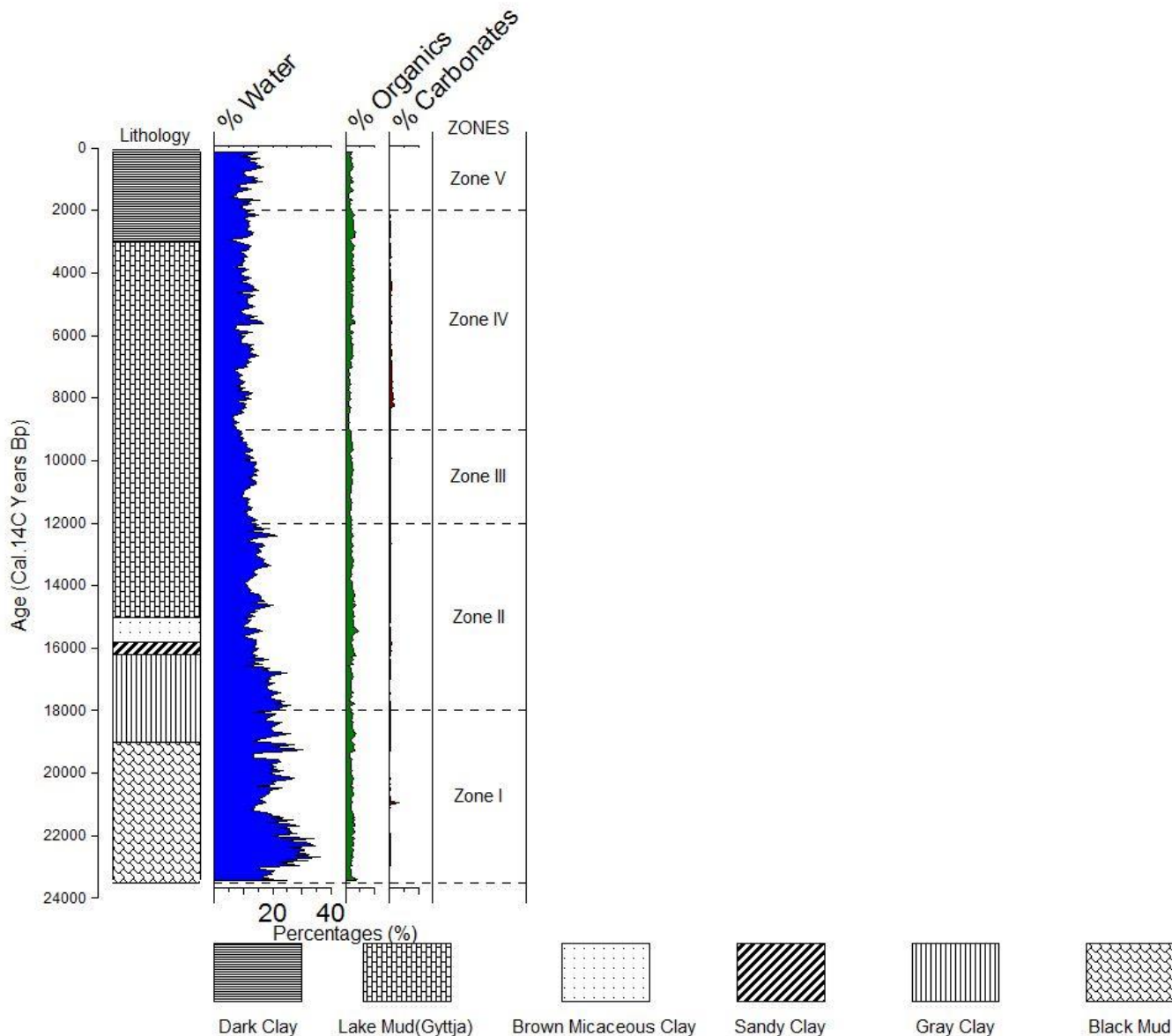


Figure 6: Sediment LOI and Lithostratigraphy data of the Kapkanyar Core Showing percentage (%) water, organics, carbonates patterns with their relative C14 ages and depth along the core.

3.3 Pollen

A total of 82 pollen and spore types were identified. All the pollen types were identified at least to the family level, and these were manually tallied and entered into a spreadsheet where they were sorted and transposed before being transferred and plotted on Tillia version 1.7.16 software. All levels inspected for pollen showed good pollen preservation except for two consecutive levels

in Zone IV (Figure 8) which showed very low counts of pollen. The sediment type containing these two levels was primarily clayey-sand. Special treatment was given to the Podocarpus pollen identified; since it was not easy to differentiate between *Podocarpus milanjanus* and *Podocarpus gracilior* pollen types, one curve was used to represent both of them in the pollen diagram (Fig 8). The differentiation of the Poaceae family pollen was also done based off grain morphology, exine thickness, grain diameter, and pore size to avoid confusion. *Zea* was in a separate curve and grass and bamboo were taken as one general Poaceae curve. A major challenge involved the identification of folded pollen grains.

From the pollen diagram, five major zones (Zone I- Zone V) were generated using CONISS. Closely related zones with small ranges were collapsed and merged which resulted in these zones that are consistent with the XRF and LOI data. The most important factors in consideration that are useful can be deduced by the explanation of the pollen diagram (Fig 9) and these are the temperature and rainfall conditions that are associated with each vegetation assemblage (Bakker, 1964).

Zone I (23.5Ka-18Ka) displays a dominance balance by the Afromontane pollen such as Podocarpus and Combrataceae pollen especially from around 23.5Ka to 22Ka while more herbaceous and shrub vegetation dominate from around 21Ka-18Ka BP. Zone II (18Ka-12Ka) is characterized by a resurgence of Afromontane vegetation after a drop towards the terminal stages of Zone I. This is observed to be more pronounced after around 16Ka BP. In Zone III (12ka-9ka), there is a sharp drop in the Afromontane elements after 12Ka concurrent with a drop in both herbaceous and shrub pollen types. Despite the drop in herbaceous vegetation such as Dracanaceae, Actinopteridaceae and Cucurbitaceae, a relatively sizeable amount of their pollen is still observed. Zone IV (9ka-2ka) is characterized by a lower amount of Podocarpus and other

arboreal pollen counts. At around 4Ka BP, there is a recovery of Podocarpus and Oleaceae pollen alongside that of the herbaceous Cyperaceae and Convolvaceae and shrub Poaceae and Myrtaceae vegetation. At the beginning of Zone V (2ka-0Ka) to present, there are generally higher levels of both Arboreal and herbaceous vegetation while a significant drop in shrub vegetation is observed.

Table 2: An exhaustive list of all the pollen types and spores identified in the Kapkanyar Swamp Core.

The Taxa represented in the pollen diagram (Fig 8) are in bold. The pollen types not included in the diagram are in normal font while the rest are grouped under intermediate/others. Classification by code: types(1)arboreal trees, (2)shrubs, (3)herbaceous vegetation, (4) others/intermediate, (5) spores			
Acacia(1) Actinopteridaceae(3) Adiantaceae(3) Adoxaceae(2) Amaryllidaceae Aspleniaceae(3) Amaranthus/Astereceae(3) Araliaceae(3) Anacardiaceae(2) Amaranthaceae(2) Bigoniaceae(2) Balanitaceae(1) Balsaminaceae(3) Burseraceae(2)	Corrigiola litoralis(3) Chenopodiaceae(3) Commelinaceae(3) Crassulaceae(3) Combrataceae(1) Croton(3) Dracanaceae(3) Dombeya(2) Dyopteridaceae(5) Diospyros(2)	Indeterminate(1,2,3) Juniperus(1) Justaicia(2) Lauraceae(3) Lobeliaceae(3) Leguminoscea(3) Lycopodium(5) Malvaceae(2) Macaranga(2) Mimosaceae(2) Myrtaceae(2) Ophoglossum Vulgatum(3) Oleaceae(1) Others(1,2,3)	Thymelaceae(2) Typha(3) Tylophora(3) Urticaceae(2) Ulmaceae(1) Vitacea(2) Woodsia(2) Zea(2)
Cyperaceae (3) Campanulaceae(3) Cyathea(3) Canabis(3) Caesalpinaceae(1) Celtis(2) Convolvaceae(3) Cordeauxia(2) Curcubitaceae(3) Cactaceae(3)	Euphorbiaceae(2) Erica(2) Euclea(1) Eugenia(2) Fabaceae(3) Fern(5) Ficus(2) Fraxinus(1) Grammitidaceae(2) Hagenia(1) Hymenophyllaceae(5) Hypericaceae(3) Impatiens(3) Iridacea(3)	Pennslivanica(1) Poaceae(2) Podocarpus(1) Pteridacea(2) Polypodiaceae(1) Polygonaceae(3) Rhamnaceae(1) Ranunculaceae(2) Reseda(2) Rubiaceae(2) Rutaceae(3)	

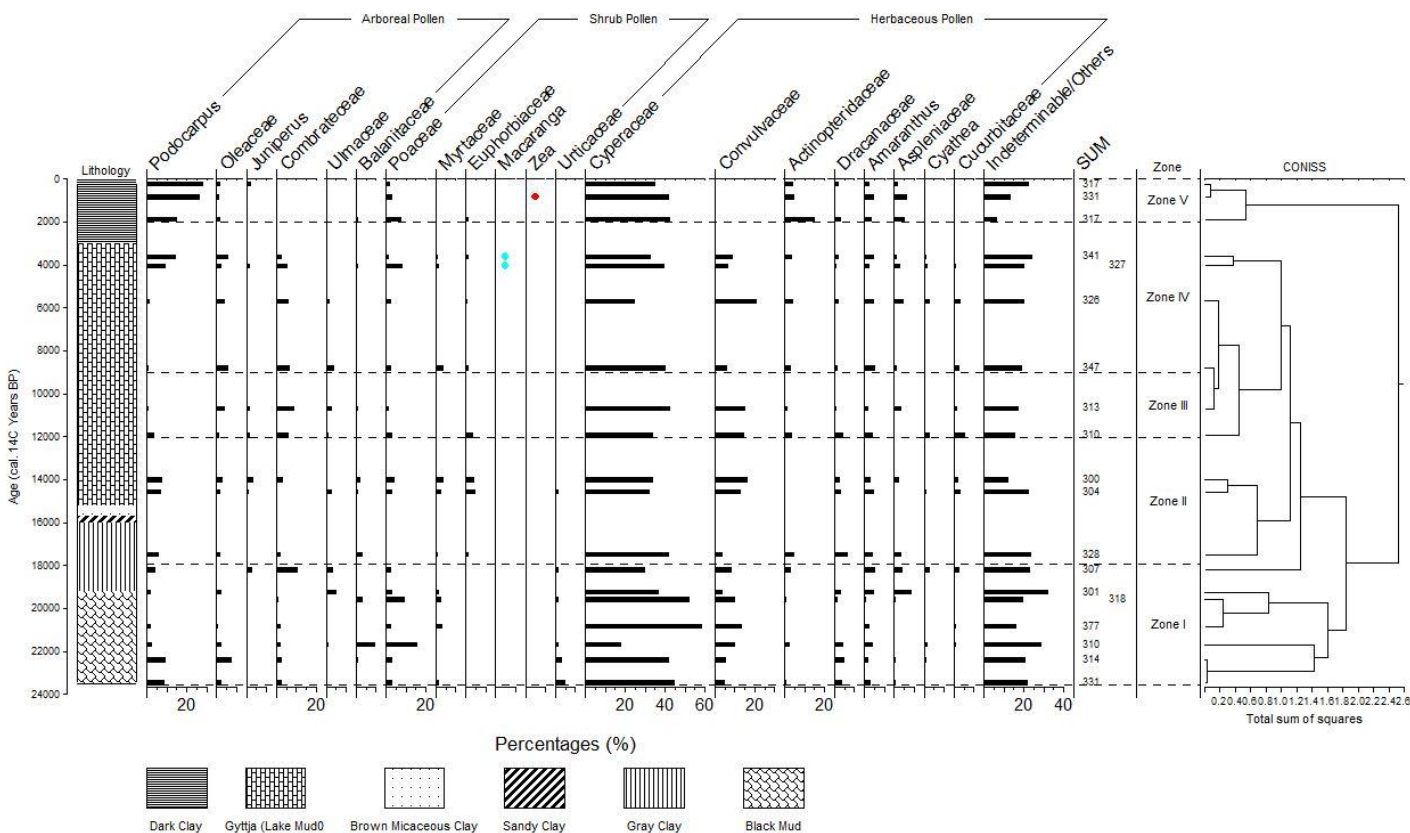


Figure 7: Pollen diagram showing percentage calculations of relative abundance of pollen with five dendrograms showing distinct pollen assemblage zonation based on the CONISS classification. The colored dots represent presence of grains below 3% threshold for representation as bars.

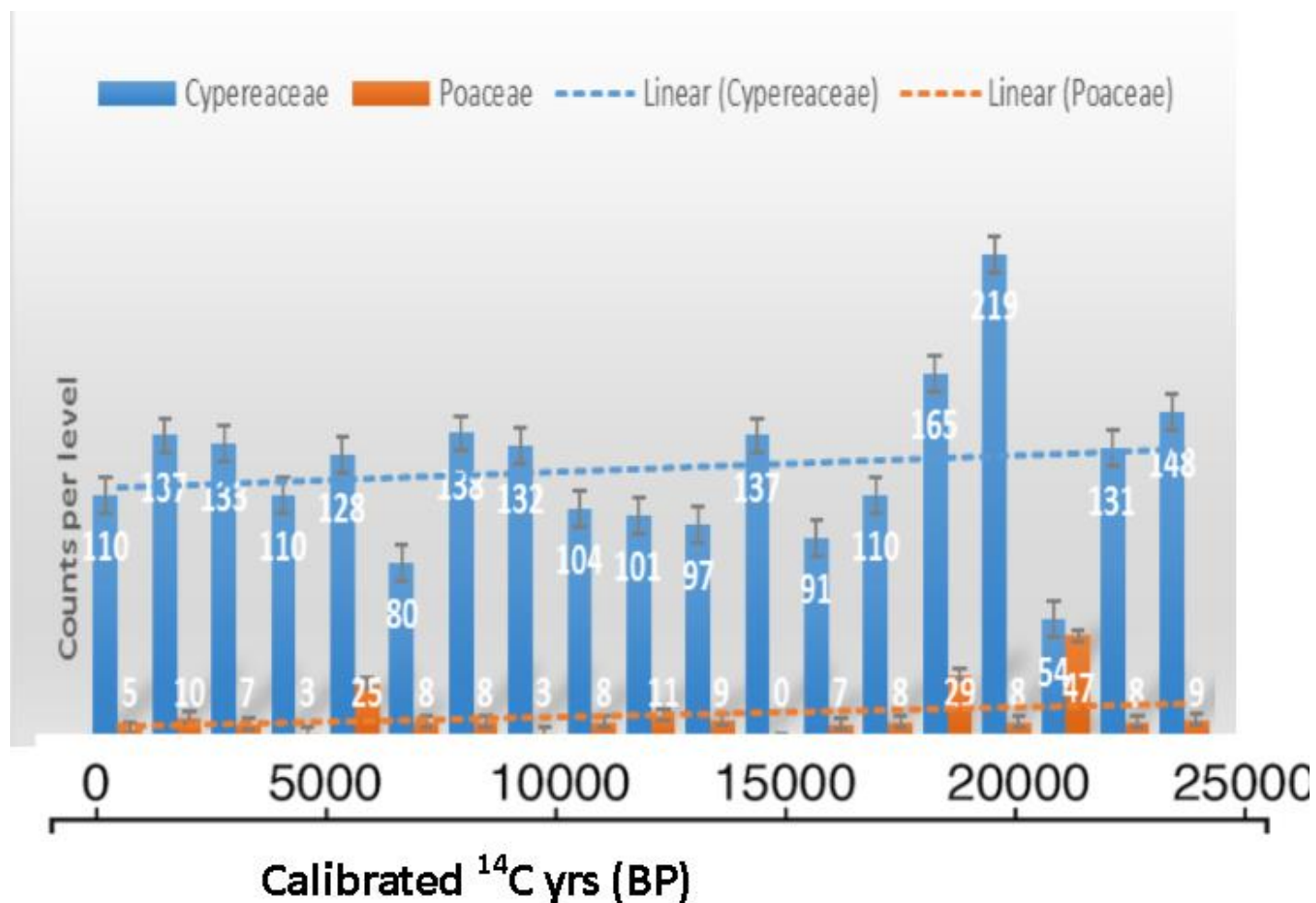


Figure 8: Illustration of wetness dynamics as depicted from the proportions of the Cyperaceae to Poaceae pollen throughout the record.(numbers on bars indicate the pollen counts).

Trend lines show a general decrease in both pollen types from the LGM to present. Cyperaceae pollen is observed to dominate throughout the wetness index spectrum. The two periods herein showing high counts of Poaceae pollen fall around 6Ka and 22Ka BP calibrated years while those showing higher values of Cyperaceae pollen are approximately 18Ka, 17Ka, 7.5Ka, 2Ka and 3kaBP in decreasing order.

3.4 Charcoal

Zones I and II are almost devoid of microscopic charcoal except for four levels that recorded negligible frequencies. Zone III shows two levels rich in microscopic charcoal, especially tree charcoal centered at ca. 10.5Ka BP. Zone IV displayed the highest microscopic charcoal count with the highest peaks of both grass and tree microscopic charcoal at around 8Ka that gradually falls with the proceeding levels and recovers at around 4ka and further drops continuing into Zone V. Charcoal from woody vegetation is observed to dominate throughout the spectrums. In some levels, only some negligible quantities (less than ten counts) per level are observed, and these were disregarded on grounds that they could be a product of contamination during processing. A general decreasing trend is observable in the charcoal counts along the core albeit with isolated peaks at two levels at around 10.5Ka and 8Ka BP which are distinctly notable with higher counts of angular elongated microscopic tree charcoal in the former and both tree charcoal and charred grass cuticles in the latter (Fig.9).

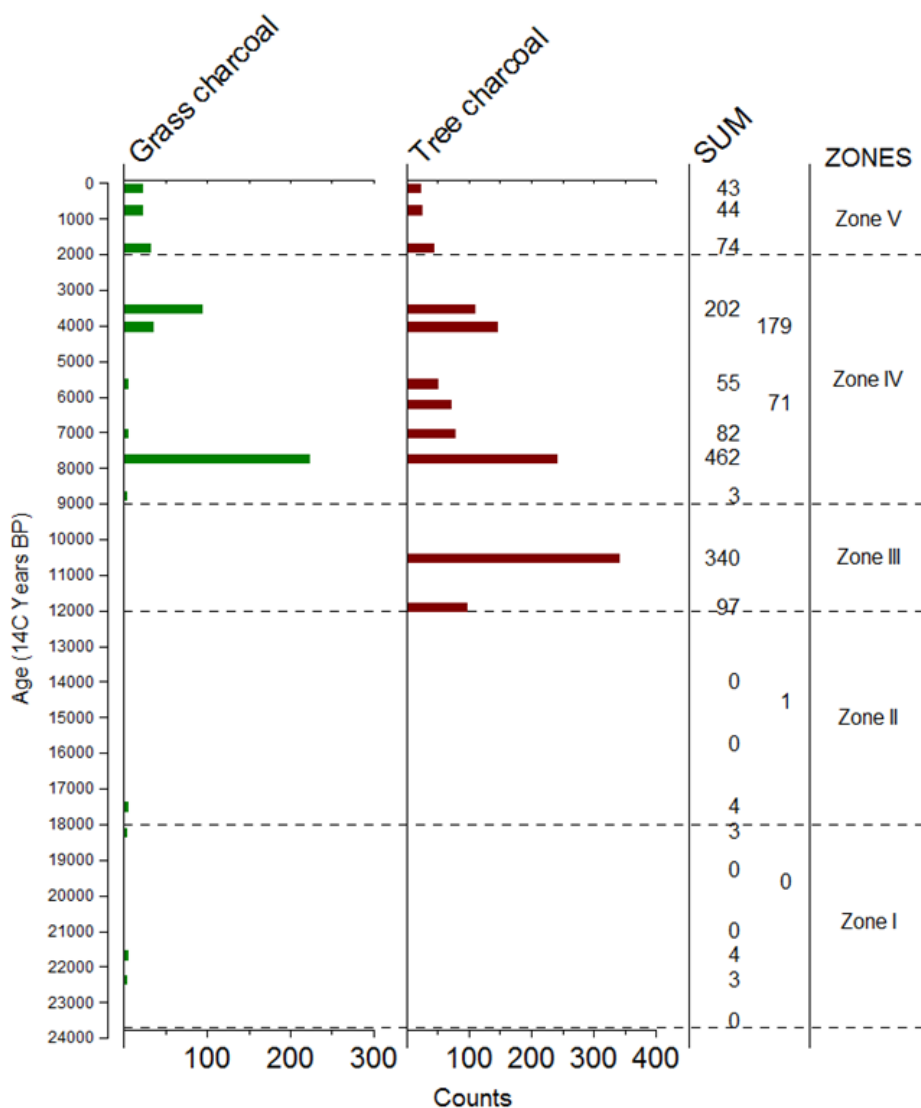


Figure 9: A figure showing charcoal representation and abundance down the Kapkanyar core used to develop possible fire regime of the Kapkanyar site.

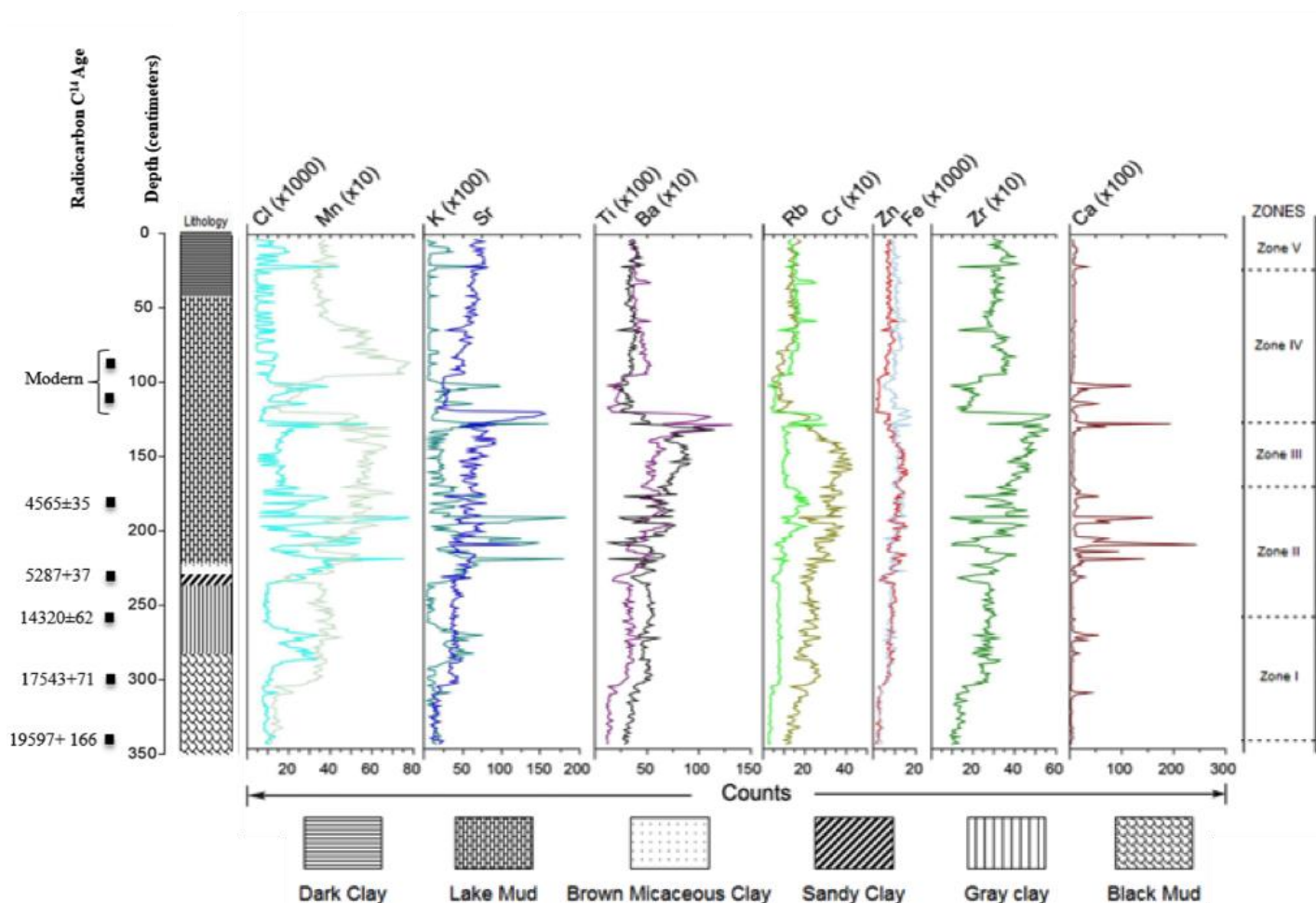


Figure 10:Kapkanyar Core XRF spectrum showing down the core concentrations of selected elements useful for paleoclimatic interpretations with changing lithology.

From the XRF spectrum plot (Fig 10), special interest is put in elements that would show variations with alterations in hydrological conditions such as Cl, Mn and K. Also, terrestrial elements such as Ti, Fe and Zr are observed to give inference to the levels of terrestrial input into the mire. Cl, K and Ca are observed to display similar trends down the core: that is for the most part parallel to the trends displayed by the terrestrial elements Ti, Zr and Fe.

Cl, K and Ca are characterized by a medium-high peak followed by a gradual decrease into a low plateau phase from (345cm-258cm) in Zone I (23.5Ka-18Ka BP) that transitions into Zone II(18Ka-12Ka) with a gradual increase to the highest peaks in the spectrum that gradually decrease

towards the end of the section (258cm -172cm). Zone III (12Ka-9Ka BP) displays smooth gradual increases in the peaks of elemental concentrations between (172cm-128cm) which is followed by a plateau phase and relative two high peaks in the last portion of section between 128cm-27cm in Zone IV (9Ka-2Ka BP). Lastly in Zone V (2Ka-0ka BP) relatively high spikes between (27cm-0cm) are observed.

Fe, Zr and Ti are generally characterized by:

- From (345cm-258cm) in Zone I (23.5Ka-18Ka BP), a medium-high plateau phase followed by a lower plateau phase that commences at around 300cm depth aged approximately 21Ka BP.
- From (258cm -172cm) in Zone II (18Ka-12Ka) relatively medium-high concentrations of the elements are observed with pulses of drops and rises.
- Between (172cm-128cm) in Zone III (12ka-9ka), the highest concentrations of these individual elements spectra are observed. This transitions to a sharp drop at 128cm in Zone IV (9ka-2ka) that is followed by a slight rise and a relatively low plateau phase between 100cm-0cm that continues into Zone V (2Ka-0ka BP).

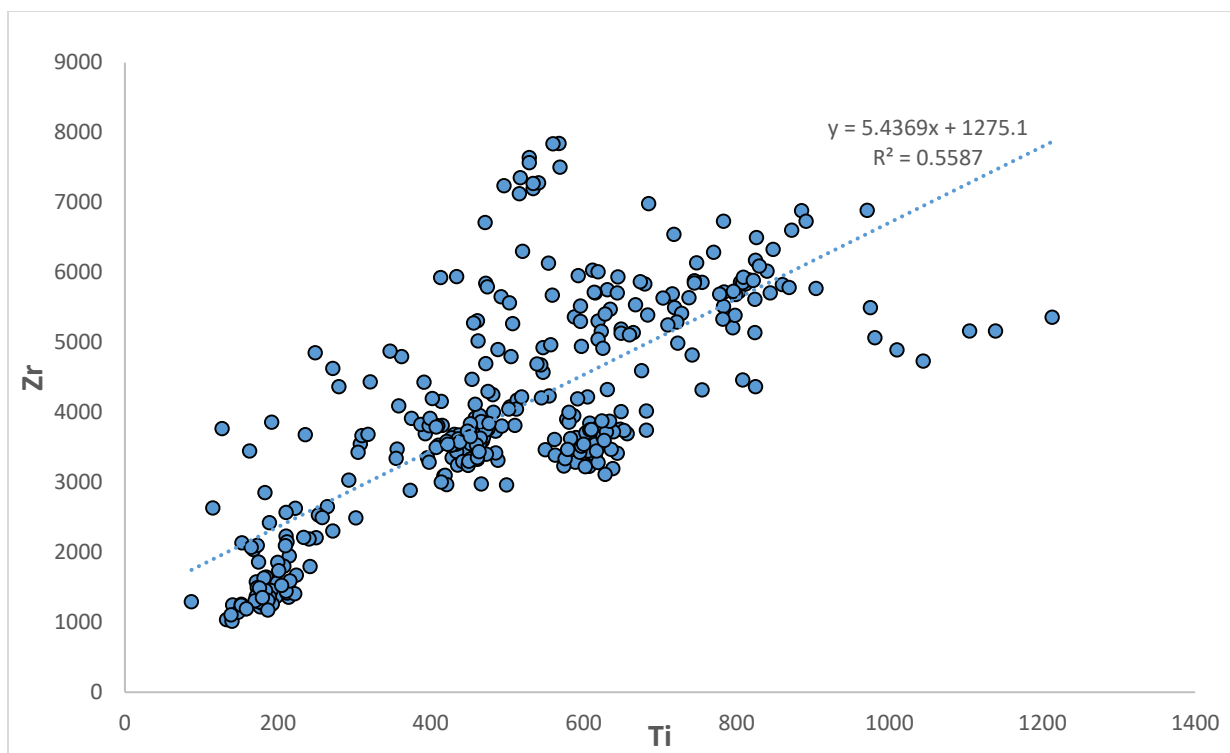


Figure 11: A matrix of correlation showing pair of elements with the highest R2 value (Zr vs. Ti)

4 DISCUSSION

The age model developed to provide timing to the chronological occurrence of events in the study, omits the 5287 ± 37 second ^{14}C age recorded at 228cm in core KAP 01 (Table 1). For the 5287 ± 37 ^{14}C at 228 cm to be accepted then we also have to accept extremely low sedimentation rates between approximately 17.5Ka BP and 5.3Ka BP, which would be inconsistent with the other dates recorded at 300cm and 345 cm. That would in turn imply anomalously high sedimentation rate between 5.3Ka-0Ka BP. Between the former mentioned ages, two levels whose matrix was majorly sandy-clay with coarse grained sand, showed exceptional low levels of pollen preservation with counts that were too low to surpass the threshold for representation in the pollen diagram (Fig 7). Although depositional circumstances could be a possible explanation for lack of preservation (Kiage et al., 2017), it could also be a product of an extreme drought event which deprived the environment of moisture which plays a decisive role in pollen preservation (Coetzee, 1967). This could invoke more research to check if this was a nonconformity resulting in a period of no deposition hence a hiatus.

The combination of the paleoenvironmental proxies used greatly complemented each other and aided to pinpoint hotspot time windows to focus on as periods of significant ecosystem responses to climatic variability through the LGM, the late glacial transition and the Holocene. Different expressions of the pluvial and arid periods have been manifested differently in different papers, but herein, seasonal distribution of precipitation which has been often correlated to wind system seasonal shifts in the region through the years (Coetzee, 1967; Oettli and Camberlin, 2005) was the main focus for clear inferences to be surmised. Emplacing the plots of the pollen diagram, the XRF spectrum and the LOI data adjacent to each other, a reliable climate history is deduced founded on several robust and dependable proxies.

Zone I of the pollen diagram covers 23.5Ka-18Ka BP that mostly represents the LGM. This zone is characterized by high levels of dry montane rain forest vegetation such as Podocarpus and Oleaceae. Zone I also showed relatively high frequencies of Poaceae and Asteraceae pollen types. The low representation (<3%) of Hagenia pollen in the Cherangani record is somewhat unusual considering records from most East African mountains such as Mount Kilimanjaro and Mount Kenya (Coetzee, 1967; Rucina et al., 2009) that have high representations of Hagenia components. However, it is possible that the low altitudinal location core site for this study meant that the Cherangani Hills may have failed to effectively record vegetation components of the altitudinal Bamboo Zone and the montane rain forest vegetation belts represented in Mt. Kilimanjaro and Kenya. Zone I is also characterized by relatively high organic content while the carbonate levels are largely unremarkable. The content of the black mud in this basal zone of the core dated 19.5Ka BP and calibrated to 23.5Ka BP, is interpreted as the first deposits to be mixed with the glaciers in this record. This level contains a mixture of both Afromontane vegetation elements and Ericaceae belt elements alongside drought indicator pollen such as Amaranthus pollen of the Asteraceae family and a high count of aquatic Cyperaceae pollen. It is possible that the pollen content in the sediment towards the end of the zone (at ca.18Ka) could be a mix of materials released as the glaciers melted and not the original vegetation at the particular point in time. However, the patterns exhibited are in tandem with the period of treeless vegetation in the Kaisungor record (Coetzee, 1967) represented by the increases in Compositae pollen values and the inferred cold and moist period (Kiage and Liu, 2006) between 30Ka and 21Ka BP and the period succeeding it which was around 2°C colder. The patterns exhibited are generally common of a cold and moist climate.

Zone II (18Ka-12Ka) mainly covers the late glacial transition period. Profound patterns are exhibited between 19Ka and 16Ka BP. Between 19Ka and 17.5Ka there is a drop in Afromontane vegetation such as Ulmaceae, Combrataceae and Podocarpus and a relative resurgence in Asteraceae pollen with a very small representation of Erica pollen. The presence of the Erica pollen from the Ericaceae family alongside the relative high values in Asteraceae pollen suggests that this period was cold and dry. This period lines-up with the upsurge in terrestrial elements of Fe, Zr and Ti in the XRF spectrum (Fig 10). All these patterns are concomitant with a Heinrich stadial event during the glacial termination (Denton et al., 2010). This period has been noted in (Hamilton, 1982) as the period of world ice volume maximum which greatly reduced the moistness of the air masses affecting the East African region. Towards 17Ka BP, an appreciable percentage increases in Afromontane pollen types as depicted in (Fig 7) and a relative increase in wetness from the wetness index (Fig 8) are noted. This is further supported by an increase in organics and water percentages in LOI data (Fig 6). The recovery of dry montane rainforest vegetation such as Olea pollen and Podocarpus at around 17Ka BP following a drop between 19Ka and 17.5Ka can be considered a response to high humidity and temperatures amelioration at the commencement of this period that marked the transition stage of the LGM. This could be an indication of a localized increase in precipitation for which dynamical reasons may not be apparent. A possible explanation is given for this phenomena as the activity of the East African Monsoon when the compression of the ITCZ towards the equator by the increase in Antarctic Sea Ice coverage and sizeable Northern Hemisphere ice sheets that plunged the easternmost part of tropical Africa into a wet period (Chiang and Bitz, 2005; Tierney et al., 2011). The enlargement of the Antarctic ice-sheet might have exerted high pressures on the North-West Europe ice-cap that consequently depressed the route of the Westerlies down across North-Africa and further southwards resulting in increased

rainfall (Bakker and Maley, 1979). However, Coetzee (1967) observed that the ITCZ activities are quite difficult to detect, particularly the disturbances necessary to activate the convective processes, which consequently makes it difficult to account for climates during such transitions. The period spanning 16Ka -12Ka BP show similar proxy patterns as those described towards ca. 17Ka, these patterns indicate a humid and moist period with the former age marking the beginning of the African Humid period at around 16Ka (Foerster et al., 2012; Liu et al., 2017; Wright, 2017; Zielhofer et al., 2017). Massive scale world ice melting occurred during this period that released enormous amounts of water into the oceans.

In Zone III (12Ka-9Ka BP), the relative frequency of the Poaceae pollen is very high. In deed the period just before 12Ka BP was characterized by a significant drop in the levels of both water and organics and a slight rise in carbonates. These patterns appear to be synchronous with the occurrence of the Younger Dryas event that is noted in most literature (Foerster et al., 2015; Wright, 2017), which is a possible explanation of this phenomenon that is common of an episodic hot and dry climate. The Younger Dryas aridity event has been marked by a substantial increase in Graminae pollen in the Ruwenzori and Kaisungor pollen diagrams by (Coetzee, 1967). This period was noted as a cold period in North West Europe as the upper Dryas stadial where the re-advancing of some glaciers hampered the general climatic warming (Hamilton, 1982).

Zone IV (9ka-2Ka BP) covers the early Holocene period into the late Holocene. At ca. 9Ka BP there is a sharp drop in the levels of both water and organics that are accompanied by a spike in the level of carbonates which can be interpreted as a major drought event that led to a significant increase in the level of siliciclastic sediments when the mire might have dried up due to the existing climate conditions. This is further supported by an influx in terrestrial elements denoted by spikes in the Fe, Ti and Mn spectra in the elemental XRF spectrum. Some of the intermittent aridity

experienced during the African humid period could be associated with the cooling event in the Northern Hemisphere that resulted in the southward shift of the ITCZ. The aridity pulses around 10.5Ka and 8.5Ka BP in the record were accompanied by two significant fires events which are possibly natural fires given the intensity of the two fires inferred from the higher counts of both grass and tree charcoal (Fig 9) and the scale inferred from the count, size and shape of the charcoal particles. Charcoal particles in these two fire events are observed to have a high count, are large, elongated, and angular in shape, which is characteristic of a widespread fire (Aleman et al., 2013b; Burney, 1987; February, 2000) that would be common in dry conditions vegetation covering vast areas of land. Aridity conditions are ideal environments for such types of fires with the availability of biomass and a spark source that could possibly be lightning. Despite these dry pulses in the record, the early to the mid-Holocene period in East Africa is depicted as having been confined by wet conditions which is consistent with the period of maximum insolation in the Northern Hemisphere (Liu et al., 2017)

Similar trends are observed in three periods in this zone: around 6Ka BP that could be associated with the termination of the African Humid Period (AHP) that plunged the East African region into a desiccation pulse. The termination of the AHP can be attributed to the termination of two fundamental mechanisms that controlled wetness in the AHP, that is, the Northern Hemisphere insolation that significantly raised the Atlantic Ocean Moistures and the addition of moisture from the Indian Ocean (Liu, et.al, 2017). The accuracy of termination of the AHP has been seen to vary in different literature material most likely due to the contrasting resolutions of the various proxies employed (Liu et al., 2017). This drought event is corroborated by the wetness index diagram (Fig 8) where Poaceae values are observed to be high possibly indicating a period of increased grassland cover during the late Holocene period.

Another notable drought event occurred around 4Ka-3.5Ka BP as observed and discussed in several records (Annie et al., 2007; Kiage et al., 2017; Rucina et al., 2009; Sánchez Goñi et al., 2017). This desiccation event is marked by a high count of the *Podocarpus* pollen and the *Olea* pollen type accompanied by a relative increase in Poaceae and Asteraceae pollen. This desiccation event is noted in the Kapkanyar core by an increase in siliciclastic sediments in the LOI diagram (Fig 6) and an increase in terrestrial sediments such as Mn, Ti and Fe (Fig 10).

In different records, this event conforms with the commencement of the imprints of anthropogenic activities (Wright, 2017). It has been recorded as an increase in Millennial-scale sub-Saharan dust in Zielhofer et al., (2017) which is also recorded as a peak in atmospheric dust presumably of Saharan origin in the deep-sea cores from North East Atlantic in Parkin and Shackleton (1974) and a spike in *Olea* and *Podocarpus gracilior* which are both good indicators of dry conditions (Coetzee, 1967; Garcin et al., 2012; Marchant et al., 2018). Although this event has also been associated with human impact, the fact that it is on an orbital scale negates the validity of the argument on the basis that if it was only human induced it would only be limited to a few pockets of the globe where populations were dense. Hence supporting the argument that the drought pulse in the record was associated to a combined impact of anthropogenic activities and a telecommunication event such as the equatorward movement and intensification of the subtropical anticyclones (Hamilton, 1982).

Considering the occurrence of charcoal and the radiocarbon chronology (Table.1), there is an increase in the frequency of the fire events especially at around 4Ka BP (Fig 9) and a reduction in the arboreal vegetation with an increase in Poaceae pollen (Fig 7). The presence of the *Macaranga* pollen of the Euphorbiaceae family that is identified as an obligate heliophytic plant type also is an indication of a more open type of forest possibly with no canopies. This supports

the postulation that the region was mostly made of vast grasslands that could possibly be a product of forest fires given a hot and dry enabling environment and spark sources which could range from natural mostly lightning to human-instigated possibly from fire hunting techniques, honey harvesting or as control of pests such as tsetse flies (*Glossina*).

The third notable drought period is at 2.5Ka which correlates with the occurrence of the “Arsi” drought event recorded in a sediment record from Ethiopia (Foerster et al., 2015), which resulted in substantial drying. Decreases in concentration of elements such as Mn and Cl also could suggest evidence of hydrological alterations (Liu et.al, 2018) during these aridity events. Dominance of the Ti signal over the Zr signal is also observed to fall concomitantly with these aridity periods. This could be indicative of an increase in terrigenous sediments runoff during such periods (Martinez-Ruiz et al., 2015; Reotita et al., 2014). Generally, the elemental concentrations (Fig 10) show a trend of increases in terrestrial elemental concentrations (Ti, Fe and Mn) to be concomitant with transitions from a more mesic phase to these drier phases.

In Zone V (2ka-0KaBp), from the lower boundary of 2Ka BP to ground surface (present), a general resurgence of both Arboreal and herbaceous vegetation accompanied by a significant drop in shrub vegetation is observed. Evidence of human imprints in this zone is further supported by presence of the *Zea* pollen that shows an introduction of agricultural activities. Specific keenness was employed as to the diameter of the grains to ensure that the *Zea* pollen (>45 µm-122 µm) were not confused for grass (37 µm -50 µm) or bamboo (30 µm-40 µm) pollen that are of similar morphology. The first occurrence of *Zea* in this record is at approximately 2Ka years BP, but this is contentious since the introduction of *Zea* by the Portuguese in Africa was dated in the 16th century around 1502 in the West African coast and later to the interior of the continent and later at around 1530 in the East African Coast where *Zea* was formerly known as *Milho zaburro*

(*Miracle, 1965*). This was roughly 500 years from the present. Also, the number of grains counted in this level was only 3 grains that is very low and thus leading to the deduction that this was probably a product of contamination during pollen processing or even compaction over time. *Zea* grains are rather large and would not easily be transported into the mire: the age/depth relationship at such a shallow depth may hence also be effected by compaction or lack thereof. Shallow soft sediments that formed the top portion of the core, are prone to compaction as compared to deeper more compacted sediments. This was thus not represented in the pollen diagram.

The presence of the human imprints through agriculture explains the resurgence of the arboreal and herbaceous vegetation that could be possibly as a result of more controlled burning through policies of forest protection and also from the establishment of firebreaks that are a product of human activities such as land partitioning in their efforts to fragment land for agriculture and settlement.

The reduction in forest fires indicated by the observation of low microscopic charcoal counts in this section of the record at the beginning of Zone V also corroborates the argument of more controlled fires. This is further complemented by the LOI data that shows an abundance of organics and water content in the sediments and a very low plateau phase of carbonates. The elemental XRF data on the other hand shows relatively high levels of elemental Cl, Zr and Mn and a decrease in all other terrestrial elements such as Fe and Ti within this zone. All these parameters are indicative of more mesic conditions (Colombaroli et al., 2016). The climate around this time can be firmly surmised to have been wetter than that between 6Ka BP-3Ka BP.

Profound vegetation shifts consequent of environmental changes are observed to have taken place in the past from the fossil pollen data. As compared to other records (Courtney Mustaphi et al., 2017; Marchant et al., 2018) that show a documentation of a high magnitude of

the climatic changes in the fossil pollen record, the Kapkanyar core shows a lower magnitude of environmental changes in palynology but dynamics of arid and pluvial periods are observed the other supporting paleoenvironmental proxies.

In the wetness index illustration (Fig 8) Cyperaceae pollen dominates throughout the spectrum; this can be explained by the fact that it is common in a mesic environment, which is typical of a swamp or mire. This is described (Coetzee, 1967) as an abundance of aquatic pollen that is indicative of local edaphic soil moisture. Trend lines in the wetness index show a general increase in wetness from the LGM to present. This closely supports the record of the millennial and other sub-orbital scale perturbations in climate as it swung from a reasonably cold and moist LGM to a humid early Holocene (Berke et al., 2014). Human imprints are strongly confirmed in Zone V and are observed and exposed as the dominant force driving regime change in the late Holocene period in general.

The fact that most of the East African region is characterized by variations in topography of landscapes (Oettli and Camberlin, 2005) generally results in significant heterogeneity due to differences in microclimates and macroclimates (Coetzee, 1967) that can be created in different areas depending on the relief settings hence the lack of a monotonous climate trend that can be representative of the whole region. This phenomenon could explain why some of the observations in the Kapkanyar core may not fully conform to observations from previous studies (Foerster, 2012; Bakker, 1964; Coetzee, 1967) that show transitions from an arid-glacial Pleistocene into a humid post-glaciation period compared to an early moist-glacial to a late arid-glacial to a humid post-glacial Holocene which is depicted in the Kapkanyar record. Such disparities call for more paleoecological research in the region. Such investigations from multiple sites would act as paleo-

weather stations, which could yield a more representative understanding of the different climatic variations and transitions that have occurred in the whole East African region.

The global climatic signals observed in the Cherangani Hills record can be surmised to be a precipitate of the climatic temperature changes during the late Pleistocene and the Holocene that were of global scale (Mustaphi, 2017; Ringard, 2016; Rucina, 2009; Tierney, 2011). This is an indication that although anthropogenic activities have greatly altered the tropical African climates, they do not completely supplant the effects of natural background climatic regime changes. Most of the paleoenvironmental and paleoclimatic deductions made herein are however in broad accord with most previously published pollen records from the East African region (Courtney Mustaphi et al., 2017; Ivory and Russell, 2016; Kiage and Liu, 2006).

5 CONCLUSIONS

The Kapkanyar core reveals substantial environmental and climatic changes at the site over the last 23.5Ka BP. The climatic variations in the record are associated with changing energy budgets of the earth. The dynamics and shifts in the proxies' relations shed light on the preexisting edaphic moisture conditions and climates given that soils are a product of climate. The East African climate is showing transition from a cold and moist LGM in the early Pleistocene, and this is later replaced by a dry-glacial phase in the late Pleistocene and followed by a wet phase with other intermittent pulses of desiccation. It is also evident from our late Pleistocene to Holocene record that anthropogenic fires are a principal periodic source of disturbance. This observation is apparent especially in the period spanning the late Holocene where fire occurrence frequency is observed to have increased. The East African Monsoon activity that is resultant of shifts in wind systems is also noted to be one of the principal controls of the climate of the East African region, which can be inferred from the precipitation patterns that have been deduced from the fossil pollen patterns in the Kapkanyar core. Although anthropogenic activities have in recent times greatly altered the East African Region Climate, they do not completely supplant the effects of natural climatic regime changes and this is supported by the global climatic temperature changes signals during the Pleistocene and Holocene that have been observed from the Kapkanyar core.

REFERENCES

- Aleman, J.C., Bentaleb, I., Blarquez, O., Bonte, P., Brossier, B., Carcaillet, C., Gond, V., Gourlet-Fleury, S., Kpolita, A., Lefevre, I., Oslisly, R., Power, M.J., Yongo, O., Bremond, L., Favier, C., 2013a. Tracking land cover changes with sedimentary charcoal in the Afrotropics. *The Holocene*, 1853-1862.
- Aleman, J.C., Blarquez, O., Bentaleb, I., Bonté, P., Brossier, B., Carcaillet, C., Gond, V., Gourlet-Fleury, S., Kpolita, A., Lefèvre, I., Oslisly, R., Power, M.J., Yongo, O., Bremond, L., Favier, C., 2013b. Tracking land-cover changes with sedimentary charcoal in the Afrotropics. *The Holocene* 23, 1853-1862.
- Annie, V., Yannick, G., Guillaume, B., 2007. Influence of Rainfall Seasonality on African Lowland Vegetation during the Late Quaternary: Pollen Evidence from Lake Masoko, Tanzania. *Journal of Biogeography* 34, 1274-1288.
- Bakker, E.M., 1964. A pollen diagram from equatorial Africa, Cherangani Kenya. *Geologie en Mijnbouw*, 123-128.
- Battistel, D., Argiriadis, E., Kehrwald, N., Spigariol, M., Russell, J.M., Barbante, C., 2017. Fire and human record at Lake Victoria, East Africa, during the Early Iron Age: Did humans or climate cause massive ecosystem changes? *The Holocene* 27, 997-1007.
- Beaudoin, A., 2003. A comparison of two methods for estimating the organic content of sediments.
- Berke, M.A., Johnson, T.C., Werne, J.P., Livingstone, D.A., Grice, K., Schouten, S., Sinninghe Damsté, J.S., 2014. Characterization of the last deglacial transition in tropical East Africa: Insights from Lake Albert. *Palaeogeography, Palaeoclimatology, Palaeoecology* 409, 1-8.
- Burney, D.A., 1987. Late Quaternary stratigraphic charcoal records from Madagascar. *Quaternary Research*, 274-278.

- Bush, M.B., Colinvaux, P.A., 1990. A pollen record of a complete glacial cycle from lowland Panama. *Journal of Vegetation Science* 1, 105-118.
- Chiang, J.C.H., Bitz, C.M., 2005. Influence of high latitude ice cover on the marine Intertropical Convergence Zone. *Climate Dynamics* 25, 477-496.
- Coetzee, J.A., 1967. Pollen analytical studies in Eastern and Southern Africa. *Palaeoecology of Africa*, 1-46.
- Colombaroli, D., van der Plas, G., Rucina, S., Verschuren, D., 2016. Determinants of savanna-fire dynamics in the eastern Lake Victoria catchment (western Kenya) during the last 1200 years. *Quaternary International*.
- Courtney Mustaphi, C.J., Gajewski, K., Marchant, R., Rosqvist, G., 2017. A late Holocene pollen record from proglacial Oblong Tarn, Mount Kenya. *PLOS ONE* 12, e0184925.
- Denton, G.H., Anderson, R.F., Toggweiler, J.R., Edwards, R.L., Schaefer, J.M., Putnam, A.E., 2010. The Last Glacial Termination. *Science* 328, 1652.
- Faegri, K., Iversen, J., 1989. *Textbook of pollen analysis*. The Blackburn Press, Caldwell.
- February, E.C., 2000. Archaeological charcoal and dendrochronology to reconstruct past environments of southern Africa. *South African Journal of Science* 96, 111-116.
- Foerster, V., Junginger, A., Langkamp, O., Gebru, T., Asrat, A., Umer, M., Lamb, H.F., Wennrich, V., Rethemeyer, J., Nowaczyk, N., Trauth, M.H., Schaebitz, F., 2012. Climatic change recorded in the sediments of the Chew Bahir basin, southern Ethiopia, during the last 45,000 years. *Quaternary International* 274, 25-37.
- Foerster, V., Vogelsang, R., Junginger, A., Asrat, A., Lamb, H.F., Schaebitz, F., Trauth, M.H., 2015. Environmental change and human occupation of southern Ethiopia and northern Kenya during the last 20,000 years. *Quaternary Science Reviews* 129, 333-340.

- Garcin, Y., Melnick, D., Strecker, M.R., Olago, D., Tiercelin, J.-J., 2012. East African mid-Holocene wet–dry transition recorded in palaeo-shorelines of Lake Turkana, northern Kenya Rift. *Earth and Planetary Science Letters* 331-332, 322-334.
- Gasse, F., 2000. Hydrological changes in the African tropics since the Last Glacial Maximum.
- Ivory, S.J., Russell, J., 2016. Climate, herbivory, and fire controls on tropical African forest for the last 60ka. *Quaternary Science Reviews* 148, 101-114.
- Izumi, K., Lézine, A.M., 2016. Pollen-based biome reconstructions over the past 18,000 years and atmospheric CO₂ impacts on vegetation in equatorial mountains of Africa. *Quaternary Science Reviews* 152, 93-103.
- Kiage, L.M., Howey, M., Hartter, J., Palace, M., 2017. Paleoenvironmental change in tropical Africa during the Holocene based on a record from Lake Kifuruka, western Uganda: PALEOENVIRONMENTAL CHANGE IN TROPICAL AFRICA. *Journal of Quaternary Science* 32, 1099-1111.
- Kiage, L.M., Liu, K.-b., 2006. Late Quaternary paleoenvironmental changes in East Africa: a review of multiproxy evidence from palynology, lake sediments, and associated records. *Progress in Physical Geography: Earth and Environment* 30, 633-658.
- Kiage, L.M., Liu, K.-b., 2009. Palynological evidence of climate change and degradation in the Lake Baringo area, Kenya, East Africa since AD 1650. *Palaeogeography, Palaeoclimatology, Palaeoecology*, 60-72.
- Liu, X., Rendle-Bühning, R., Kuhlmann, H., Li, A., 2017. Two phases of the Holocene East African Humid Period: Inferred from a high-resolution geochemical record off Tanzania. *Earth and Planetary Science Letters* 460, 123-134.

- Marchant, R., Richer, S., Boles, O., Capitani, C., Courtney-Mustaphi, C.J., Lane, P., Prendergast, M.E., Stump, D., De Cort, G., Kaplan, J.O., Phelps, L., Kay, A., Olago, D., Petek, N., Platts, P.J., Punwong, P., Widgren, M., Wynne-Jones, S., Ferro-Vázquez, C., Benard, J., Boivin, N., Crowther, A., Cuní-Sanchez, A., Deere, N.J., Ekblom, A., Farmer, J., Finch, J., Fuller, D., Gaillard-Lemdahl, M.-J., Gillson, L., Githumbi, E., Kabora, T., Kariuki, R., Kinyanjui, R., Kyazike, E., Lang, C., Lejju, J., Morrison, K.D., Muiruri, V., Mumbi, C., Muthoni, R., Muzuka, A., Ndiema, E., Kabonyi Nzabandora, C., Onjala, I., Schrijver, A.P., Rucina, S., Shoemaker, A., Thornton-Barnett, S., van der Plas, G., Watson, E.E., Williamson, D., Wright, D., 2018. Drivers and trajectories of land cover change in East Africa: Human and environmental interactions from 6000 years ago to present. *Earth-Science Reviews* 178, 322-378.
- Martinez-Ruiz, F., Kastner, M., Gallego-Torres, D., Rodrigo-Gámiz, M., Nieto-Moreno, V., Ortega-Huertas, M., 2015. Paleoclimate and paleoceanography over the past 20,000 yr in the Mediterranean Sea Basins as indicated by sediment elemental proxies. *Quaternary Science Reviews* 107, 25-46.
- Mworia Maitima, J., 1991. Vegetation response to climatic change in central Rift Valley, Kenya. *Quaternary Research* 35, 234-245.
- Novenko, E.Y., Tsyganov, A.N., Olchev, A.V., 2018. Palaeoecological data as a tool to predict possible future vegetation changes in the boreal forest zone of European Russia: a case study from the Central Forest Biosphere Reserve. *IOP Conference Series: Earth and Environmental Science* 107, 012104.
- Oettli, P., Camberlin, P., 2005. Influence of topography on monthly rainfall distribution over East Africa. *Climate Research* 28, 199-212.

- Quick, L.J., Chase, B.M., Meadows, M.E., Scott, L., Reimer, P.J., 2011. A 19.5kyr vegetation history from the central Cederberg Mountains, South Africa: Palynological evidence from rock hyrax middens. *Palaeogeography, Palaeoclimatology, Palaeoecology* 309, 253-270.
- Reotita, J., Siringan, F., Zhang, J., Azanza, R., 2014. Paleoenvironment changes in Juag Lagoon, Philippines based on sedimentology, bulk geochemistry and stable isotopes and their implication to nutrification. *Quaternary International* 333, 110-121.
- Rucina, S.M., Muiruri, V.M., Kinyanjui, R.N., McGuinness, K., Marchant, R., 2009. Late Quaternary vegetation and fire dynamics on Mount Kenya. *Palaeogeography, Palaeoclimatology, Palaeoecology* 283, 1-14.
- Sánchez Goñi, M.F., Desprat, S., Daniiau, A.-L., Bassinot, F.C., Polanco-Martínez, J.M., Harrison, S.P., Allen, J.R.M., Anderson, R.S., Behling, H., Bonnefille, R., Burjachs, F., Carrión, J.S., Cheddadi, R., Clark, J.S., Combourieu-Nebout, N., Courtney-Mustaphi, C.J., Debussk, G.H., Dupont, L.M., Finch, J.M., Fletcher, W.J., Giardini, M., González, C., Gosling, W.D., Grigg, L.D., Grimm, E.C., Hayashi, R., Helmens, K., Heusser, L.E., Hill, T., Hope, G., Huntley, B., Igarashi, Y., Irino, T., Jacobs, B., Jiménez-Moreno, G., Kawai, S., Kershaw, P., Kumon, F., Lawson, I.T., Ledru, M.-P., Lézine, A.-M., Liew, P.M., Magri, D., Marchant, R., Margari, V., Mayle, F.E., McKenzie, M., Moss, P., Müller, S., Müller, U.C., Naughton, F., Newnham, R.M., Oba, T., Pérez-Obiol, R., Pini, R., Ravazzi, C., Roucoux, K.H., Rucina, S.M., Scott, L., Takahara, H., Tzedakis, P.C., Urrego, D.H., van Geel, B., Valencia, B.G., Vandergoes, M.J., Vincens, A., Whitlock, C.L., Willard, D.A., Yamamoto, M., 2017. The ACER pollen and charcoal database: a global resource to document vegetation and fire response to abrupt climate changes during the last glacial period. *Earth System Science Data Discussions*, 1-33.

- Santisteban, J.I., Mediavilla, R., López-Pamo, E., Dabrio, C.J., Zapata, M.B.R., García, M.J.G., Castaño, S., Martínez-Alfaro, P.E., 2004. Loss on ignition: a qualitative or quantitative method for organic matter and carbonate mineral content in sediments? *Journal of Paleolimnology* 32, 287-299.
- Schüler, L., Hemp, A., Zech, W., Behling, H., 2012. Vegetation, climate and fire-dynamics in East Africa inferred from the Maundi crater pollen record from Mt Kilimanjaro during the last glacial–interglacial cycle. *Quaternary Science Reviews* 39, 1-13.
- Stuiver, M., Reimer, P., F. Braziunas, T., 2006. High precision radiocarbon age calibration for terrestrial and marine samples.
- Stuiver, M., Reimer, P.J., Braziunas, T.F., 1998. High-Precision Radiocarbon Age Calibration for Terrestrial and Marine Samples. *Radiocarbon* 40, 1127-1151.
- Tian, F., Cao, X., Dallmeyer, A., Zhao, Y., Ni, J., Herzsuh, U., 2017. Pollen-climate relationships in time (9 ka, 6 ka, 0 ka) and space (upland vs. lowland) in eastern continental Asia. *Quaternary Science Reviews* 156, 1-11.
- Tierney, J.E., Russell, J.M., Sinninghe Damsté, J.S., Huang, Y., Verschuren, D., 2011. Late Quaternary behavior of the East African monsoon and the importance of the Congo Air Boundary. *Quaternary Science Reviews* 30, 798-807.
- Wright, D.K., 2017. Humans as Agents in the Termination of the African Humid Period. *Frontiers in Earth Science* 5.
- Zielhofer, C., von Suchodoletz, H., Fletcher, W.J., Schneider, B., Dietze, E., Schlegel, M., Schepanski, K., Weninger, B., Mischke, S., Mikdad, A., 2017. Millennial-scale fluctuations in Saharan dust supply across the decline of the African Humid Period. *Quaternary Science Reviews* 171, 119-135.